FTD-ID(RS)T-0665-89

FOREIGN TECHNOLOGY DIVISION

ANALYSIS OF CARBON FIBER'S X-RAY MICROSCOPIC STRUCTURE

by

Yang Yuxing, Wang Jiarong, Liu Changlin

Approved for public release;
Distribution unlimited.

HUMAN TRANSLATION

FTD-ID(RS)T-0665-89 16 August 1989

MICROFICHE NR: FTD-89-C-000687

ANALYSIS OF CARBON FIBER'S X-RAY MICROSCOPIC STRUCTURE

By: Yang Yuxing, Wang Jiarong, Liu Changlin

English pages: 13

Source: Shanghai Jiaotong Baxue Xuebao, Vol. 22, Nr. 5, 1988, pp. 20-28

Country of origin: China
Translated by: Leo Kanner Associates
F33657-88-D-2188
Requester: FTD/TQTAV/Jeffery D. Locker

PREPARED BY:

TRANSLATION DIVISION
FOREIGN TECHNOLOGY DIVISION
WPAFB, OHIO

GRAPHICS DISCLAIMER

All figures, graphics, tables, equations, etc. merged into this translation were extracted from the best quality copy available.

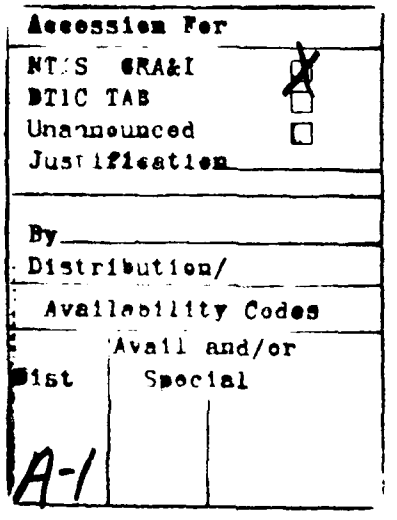

ANALYSIS OF CARBON FIBER'S X-RAY MICROSCOPIC STRUCTURE

Yang Yuxing, Wang Jiarong, Liu Changlin

TITLE: Shanghai Jiaotong Daxue Xuebao [Journal of Shanghai Jiaotong University], Vol. 22, No. 5, 1988

Pages Translated: 20-28

Words Translated: 2622

Translated No.: FTD-ID(RS)T-0665-89

Contractor: Leo Kanner Associates
P.O. Box 5187
Redwood City, CA 94063

ANALYSIS OF CARBON FIBER'S X-RAY MICROSCOPIC STRUCTURE

Yang Yuxing, Wang Jiarong, Liu Changlin,
Material Science and Engineering Department

Abstract

In this paper, we have used the X-ray diffraction method (including the small angle scatter method) to study the microscopic structure of four kinds of carbon fibers. We include the measurement of inter-layer distance C_0 for "random-layer graphite," average height L_c of layer surface stacks, average width L_a of layer surfaces, degree of orientation $W_{1/2}$, and carbon fiber's average microscopic holes. We also propose a calculation procedure for handling small angle scattering.

Key Words: Carbon fiber, graphite, microscopic structure analysis, small angle scattering.

1. FOREWORD

The structure of commonly encountered carbon fibers and graphite fibers is ordinarily "random-layer" structure [1]. It has both similarities and dissimilarities with graphite crystal. The similarities reside in the fact that both structures' layer planes are composed of six-member aromatic rings. The dissimilarities reside in the fact that in the former the carbon atoms between the layers do not have a regular, fixed position, and lack three-dimensional order, while the distance between layers is greater than in graphite crystals, reflecting the facts that the average thickness L_c of stacks of micro-crystal size on the layer surface and the average width L_a of the layer surface are also very small, and that the layer face forms a certain angle of orientation with the fiber axis. At the same time, in the "random-layer graphite" structure, in addition to the macroscopic defects, there also exists a very porous microscopic structure [2]. Because the structure of carbon fiber is one of the "random-layer graphite" structures composed of light-weight atoms that show a low degree of symmetry, even a high-resolution

---

Note in Original: This paper was received 24 October 1986.

electron microscope is not sufficient to reveal the microscopic structure's characteristics accurately and effectively. By comparison, the penetration strength of X rays is greater, the irradiated volume is larger, and the statistical quality and reproducibility are better. This paper uses large and small angle X-ray diffraction techniques for a systematic analysis of four kinds of carbon fiber microstructure.

2. LARGE ANGLE X-RAY DIFFRACTION ANALYSIS OF CARBON FIBER

A. Measurement of Carbon Fiber Lattice Constant and Degree of Graphitization

Because carbon fiber is a kind of transitional-state carbon, it is composed of amorphous carbon and thermodynamically stable crystal-state carbon (graphite). The basic structure of the most common transitional-state carbon is "random-layer graphite" structure. The layer surfaces along the axis in "random-layer graphite" can be stacked without order; there is no definite orientation (see Fig. 1). Therefore the X-ray diffraction spectra for graphite crystals and carbon fiber are obviously different (Fig. 2). In the spectra, the diffraction for face (002) is especially intense, with the inter-face distance equal to 1/2 C_0, the carbon fiber's lattice constant. Because it is extraordinarily sensitive to changes in structure, $d_{(002)}$ is often considered as an indicator for the degree of graphitization; it can be calculated from the diffraction angle of the face (002) diffraction ray. At the same time, the layer face stacking thickness L_c along the C axis can be measured from half the height and breadth of the face (002) diffraction ray. From half-breadth for the (10) or (11) ray is calculated layer plane's thickness L_a, the average thickness of stacks on the a axis direction. Based on Scherrer's formula [3], we have:

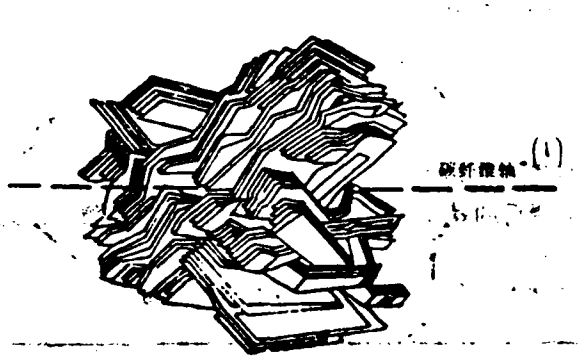

Fig. 1. Model of random-layer graphite structure. Key: (1) Carbon fiber axis.

$$L_{hkl} = \frac{K\lambda}{\beta_{hkl}\cos\theta} \quad (1)$$

in which β_{hkl} is the half breadth of the crystal surface diffraction ray after adjustment by the Rowland polarization factor, the atomic scatter factor, and the absorption factor (hkl). In the case of carbon fiber, because the micro-crystal scale is very small, the element of broadening caused by the instrument may be excluded. λ is the wave length of the X-ray, θ is the diffraction angle, K is the form factor. When measuring L_c, the value of K is approximately 1; when measuring L_a, it is approximately 1.77 [4].

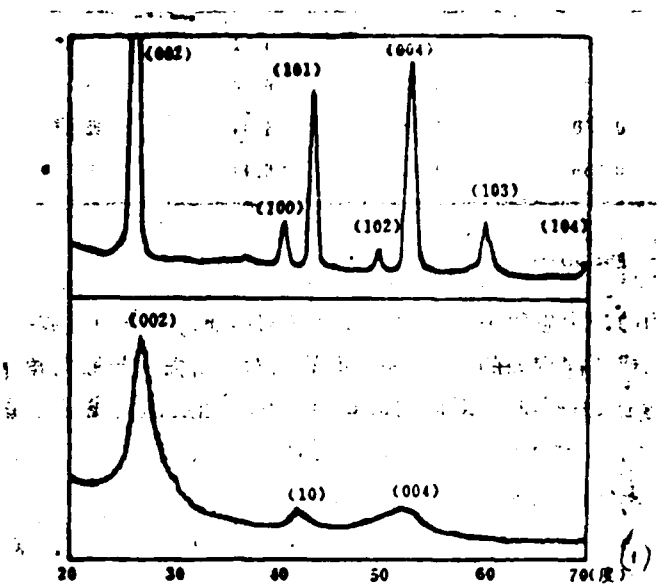

Fig. 2. X-ray diffraction spectra for graphite and carbon fiber.
a. Graphite; b. Carbon fiber processed at 1200°C.
Key: (1) Degrees.

Table 1 shows the data for the four kinds of carbon fiber: the "random-layer graphite" stack number (or micro-crystal size) obtained by wide angle X-ray diffraction analysis is a statistical average.

The higher the hot processing temperature, the larger the micro-crystal scale; the inter-layer distance is correspondingly reduced and approaches the ideal graphite crystal value, and the carbon layer structure regularity also increases gradually [5]. In order to show the structural characteristics possessed by these carbon fibers during the hot processing, as well as the degree of graphitization, use is normally made of parameters such as $d_{(002)}$, L_a, L_c. The $d_{(002)}$ value for ideal graphite crystal is 0.3354 nm (3.354 Å). As the hot processing temperature rises, the carbon structure is gradually transformed in the direction of graphite structure; its $d_{(002)}$ value obviously decreases gradually, tending toward the ideal graphite crystal value. Maire and Mering are of the opinion that carbon fiber is a composite of unordered

random-layer stacks and ordered graphite stacks; it may have the probability of ideal graphite crystal structure defined as g. They propose the following formula:

$d_{(002)}=0.3354g+0.3440(1-g)$ (crystal inter-layer distance unit is nm).

When the value of g changes from 0 to 1, it shows there is a transformation from a completely random-layer structure to an ideal graphite crystal; that is, the greater the value of g, the higher the degree of graphitization [6]:

$$g=\frac{0.344-d_{(002)}}{0.344-0.3354} \qquad (2)$$

For the value of g for the four kinds of carbon fiber, see Table 1.

Because the value of $d_{(002)}$ measured by X-ray diffraction is a statistical average value for the entire carbon structure, the degree of graphitization is also a physical quantity having statistical significance.

Table 1. Data for four kinds of carbon fiber.

Specimen:	$d_{(002)}$(nm)	L_c(nm)	L_a(nm)	g(%)	$W_{\frac{1}{2}}$(度)(1)
#1, Shangtan, 1200°C	0.349	1.61	3.84	极低*(2)	16.3
#2, Shangtan, >2500°C	0.337	4.52	6.00	81	9.0
#3, Japan, 1300°C	0.350	1.62	4.34	极低*(2)	12.0
#4, Japan, >2500°C	0.336	4.32	6.44	93	8.0

*Because the value calculated from formula (2) is an extremely small negative value, the results are clearly unbelievable; they can only show that the carbon fiber is in a state of uncertain form.
Key: (1) Degrees; (2) Extremely low.

B. Measurement of the Degree of Orientation of Carbon Fiber

In the structure of random-layer graphite, the six-member aromatic-ring network surface, composed of carbon atoms, forms an orientation of a certain degree with the fiber axis. It can be obtained by measuring the relation

between the diffraction intensity corresponding to each (002) face forming different orientations with the fiber axis, and the orientation angle ϕ. When we take the intensity as half the maximum, the corresponding orientation angle less 90° (when the layer surface normal line is exactly perpendicular to the fiber axis) is considered to be the degree of orientation, shown by $W_{1/2}$ (or z^0). It is clear that, when all layer surfaces are strictly parallel with the filament axes, $W_{1/2}$ approaches 0°. Figure 3(a) is an illustration of the degree of orientation; it is only one kind of corresponding comparative method.

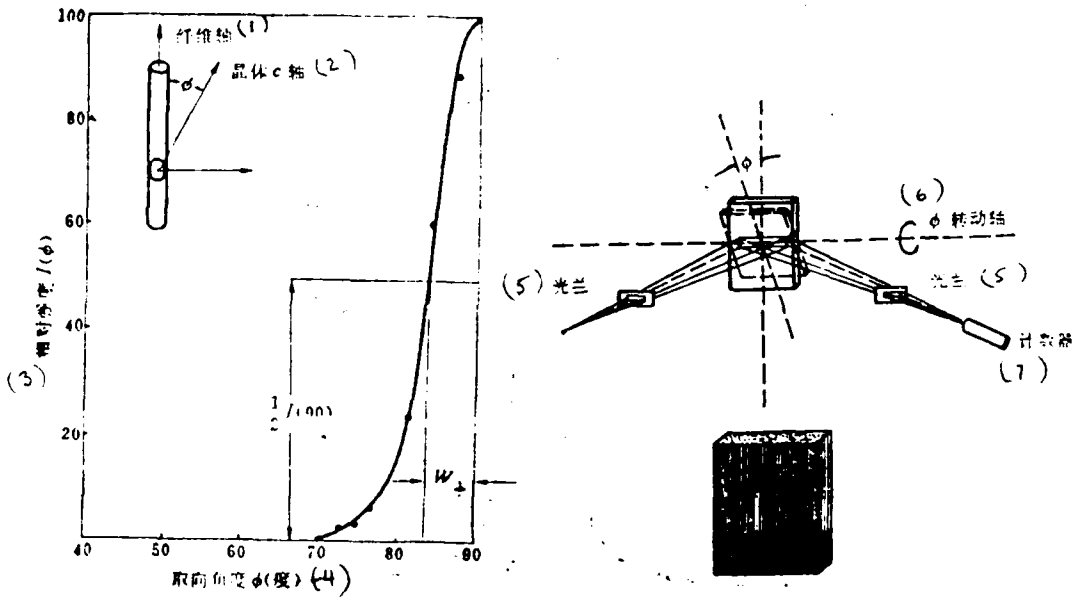

Fig. 3. (a) Illustration for angle of orientation; (b) Specimen compound of carbon fiber. Vertical orientation of carbon fiber parallel sample.

Key: (1) Fiber axis; (2) Crystal c axis; (3) Corresponding intensity $I(\phi)$; (4) Orientation angle ϕ in degrees; (5) Aperture; (6) ϕ rotational axis; (7) Counter.

When this kind of measurement is undertaken on a diffraction instrument provided with an inclined side installation, the experiment is simplicity itself: For each change of orientation angle ϕ, a measurement is taken of the diffraction peak of surface (002). Under these diffraction geometric

conditions, it is not necessary to undertake absorption corrections for the intensity [7]. Figure 3(b) is a sketch showing an inclined side installation to measure the degree of orientation. The degree of orientation $W_{1/2}$, calculated from the graph showing the relation between the intensity corresponding to face (002) and the orientation angle ϕ (see Table 1); for PAN base carbon fiber, after being graphitized at 2500°, the graphite fiber degree of orientation $W_{1/2}$ has dropped to about 8°.

3. SMALL ANGLE X-RAY SCATTER ANALYSIS OF CARBON FIBER

In addition to macroscopic defects in carbon fiber, there also appear between the layer surfaces of the "random-layer graphite" many tiny openings distributed along the axis [2]. For this reason, there exists a distinct rise and fall in electron density between "random-layer graphite" and the openings; this necessarily leads to the phenomenon of small angle scatter. Because the holes in the carbon fiber are distributed along the axis, these fiber-state holes are separated by the random-layer graphite sheets. Therefore, the small angle scatter spectra scanned perpendicularly to the carbon fiber axis and along the axis are clearly not the same. Figures 4(a) and 4(b) are respectively the perpendicularly and axially scanned small angle scatter graphs for PAN base carbon fibers which have been put through a 2500°C processing. Below, the Guinier approximation formula is used for analysis of the small angle scatter intensity graph.

(1) We deduct parasitic scattering and background (I_B). The origin of the parasitic scattering is the purity of the incident spectrum, or the scattering of the aperture, atmosphere, and other physical substances. When using a counter to measure the intensity, it is necessary to use a wave filter and a wave height analyzer, and on the basis of differences in the scatter intensity when a specimen is present and absent to reduce the influence of the parasitic scatter. Figures 4(a) and 4(b) are graphs showing the scatter intensity after the removal of parasitic scatter. It can be seen that when 2 is greater than 3°, the scatter intensity $I(2\theta)$ along with 2θ gradually approaches a steady value (background intensity I_B); as regards carbon fiber

composed of "random-layer graphite." and microscopic holes, this kind of background intensity is mainly a result of the unevenness in the interior part of the "random-layer graphite." As the graphitization becomes more nearly complete, the scale of micro-crystals in the "random-layer graphite" gradually increases; the six-member aromatic-ring network surface and the surface arrangement tend to be more intact, and the background also decreases in proportion. Obviously, this portion of the background is not part of the contribution of the microscopic holes, and so should be discounted.

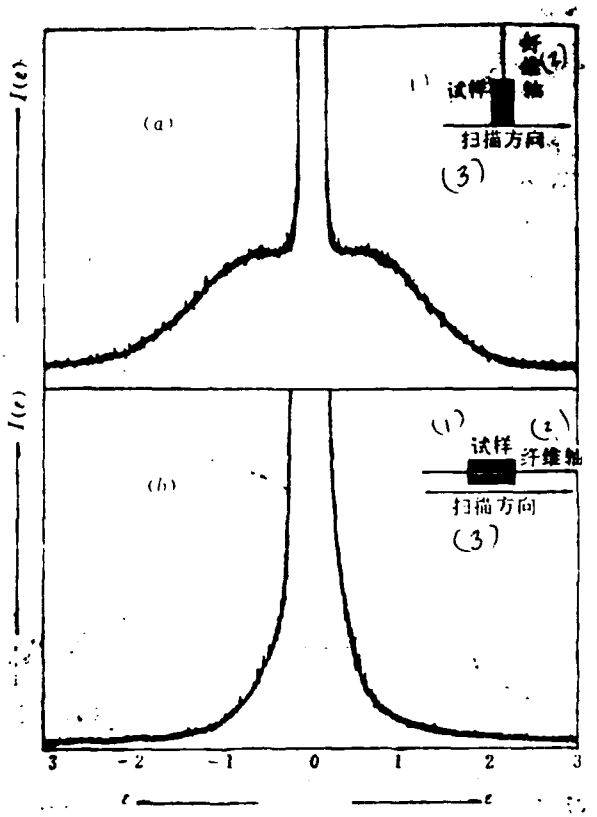

Fig. 4. Small angle scatter spectra scanned perpendicular to and along the axis.
Key: (1) Specimen; (2) Fiber axis; (3) Scanning direction.

2) Estimation of the scale of microscopic holes. When the distance between the holes in the carbon fibers is relatively great, their mutual scatter interference effect may be ignored. Based on Guinier's approximation formula [8]:

$$I(e)=M^2n\exp\left(-\frac{4\pi^2R_D^2e^2}{3\lambda^2}\right)$$

in which M is the number of microscopic holes, n is the number of electrons in one hole, ε is the small angle scatter angle, and R_D is the radius of gyration of the microscopic holes.

Substituting logarithms in both sides of the above equation, we obtain:

$$\lg I(\varepsilon)=\lg(M^2n)-\frac{4\pi^2}{3\lambda^2}R_D^2\varepsilon^2\lg e=\lg I(\alpha)-\frac{4\pi^2}{3\lambda^2}R_D^2\varepsilon^2\lg e \tag{4}$$

Making a graph of $\lg I(\varepsilon)-\varepsilon^2$, we obtain the results on Fig. 5 and Fig. 6. Figure 5 is obtained from vertical carbon fiber axis scanning; it is basically a straight line, showing that the microscopic hole radius of gyration R_D approaches a constant; from its slope it is possible to solve for R_D.

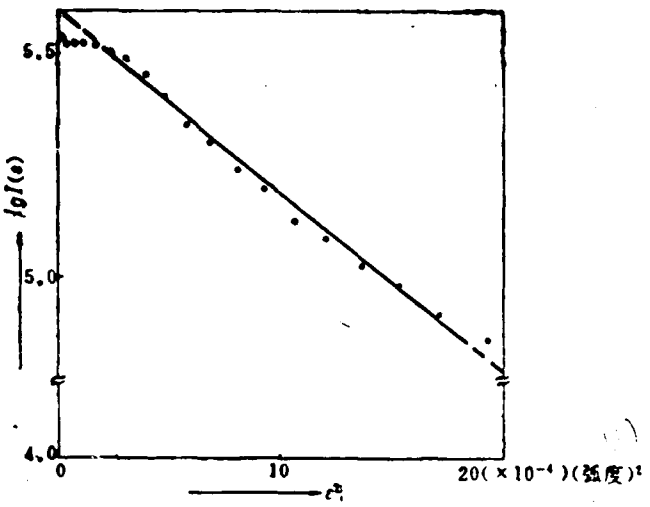

Fig. 5. Graph of $\lg I(\varepsilon)-\varepsilon^2$ obtained from scanning perpendicularly to the fiber axis.
Key: (1) Intensity

Because

$$a=-\frac{4\pi^2}{3\lambda^2}R_D^2\lg e \tag{5}$$

therefore

$$R_D=\sqrt{\frac{-3a}{4\pi^2\lg e}}\lambda=0.416\sqrt{-a} \tag{6}$$

Based on reference [2], we already know that the holes in carbon fibers are needle-form, and are distributed in parallel along the axis. From the principle of small angle scattering [8] we can determine that when scanning is undertaken along perpendicularly to the direction of the fiber axis, the diffraction geometry is as shown on Fig. 7. In this figure, $\overline{S_0}$ is the unit deviation amount of the incident beam; $\overline{S}$ is the unit deviation of the scatter ray; $\overline{H}$ is the reverse change deviation amount; $\overline{D}$ is the scanning direction. Because of the horizontal Soller fissure effect, only the scatter rays parallel with the plane determined by $\overline{S_0}$ and $\overline{D}$ can be received by the counters. It is clear that the gyration axes of the holes are perpendicular to the plane determined by $\overline{S_0}$ and $\overline{D}$, and parallel with the axis of the focal

light source and with the fiber axis. For this reason, when a given thickness is chosen for dR_D and the surface area is the micro-section dV of S_{R_D}, the function for the form contributed by the entire hole to the central diffraction peak is:

$$S(\overline{H}) = \int S(\overline{R}_D)\exp(-2\pi i\overline{H}\cdot\overline{R}_D)dR_D \quad (6)$$

Here, R_D is the radius of gyration of the micro-section; it is perpendicular to K. Based on the classical physical concept, we use the following relational formula to estimate the radius a of the needle-form hole:

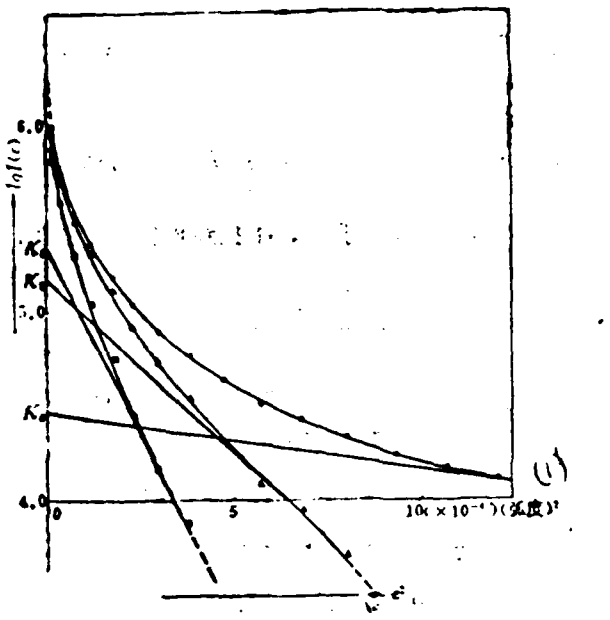

Fig. 6. Graph of $\lg I_t - \varepsilon^2$ obtained from scanning along the fiber axis.
Key: (1) Intensity.

$$R_D = \frac{1}{\sqrt{2}}a \quad (7)$$

Because R_D has no relation with the length of the needle-form hole, the hole's radius a may be calculated directly.

In order to estimate the length of the needle-form hole, it is necessary to use the scanning graph parallel to the fiber axis (Fig. 6). The corresponding diffraction geometry principle is as shown in Fig. 8. Because at this time the axis of gyration $\overline{K}$ is perpendicular to the axis of the needle-form hole, based on the classical physical concept, we use the following formula to calculate the hole's length ($2L$):

$$R_D = \sqrt{\frac{a^2}{2} + \frac{L^2}{3}} \quad (8)$$

in which a is calculated from formula (7).

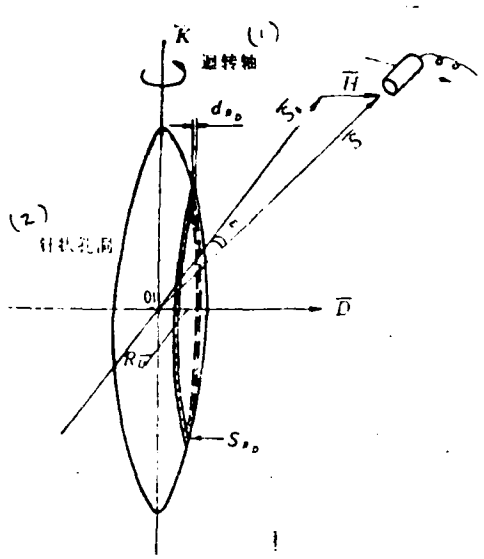

Fig. 7. Diffraction geometry when scanning perpendicularly to the fiber axis.
Key: (1) Gyration axis; (2) Needle-form hole.

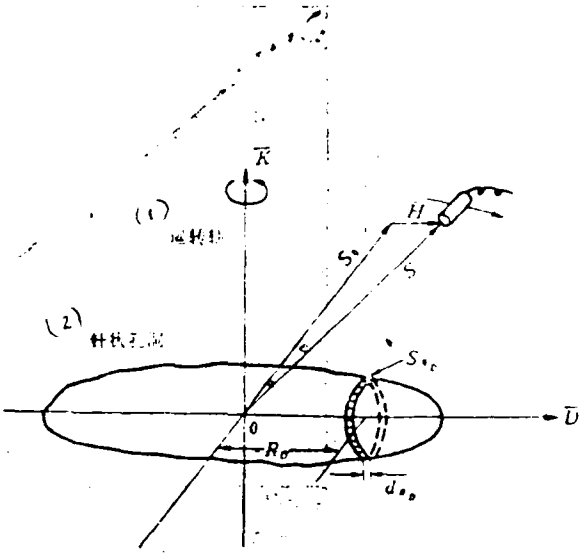

Fig. 8. Diffraction geometry when scanning along the fiber axis.
Key: (1) Gyration axis; (2) Needle-form hole.

The fact that Fig. 6 is a concave rising graph is explained by the existence in the carbon fiber of needle-form holes having gyration radii on a variety of scales. At this time, it is possible to use employ Fankuchen's grade-wise tangent method to estimate the range of their lengths. First a tangent is drawn at the portion on the graph of the greatest scatter angle, intersecting with the vertical coordinate at K_1; the slope a_1 of the tangent is then found, and after that on the original graph the intensity value shown at each point is reduced by the intensity value shown at the corresponding point on the tangent. Another $\lg I(\varepsilon)$-ε^2 graph is obtained, whereupon the same procedure is repeated. We proceed in this way by steps: Many a and K_1 values can be obtained. After they are substituted one by one into formulas (6) and (8), it is a simple matter to find their length ($2L$). Table 2 shows the scale of the holes on the four kinds of carbon fiber under consideration.

Table 2hol Range of length and radius of holes in microscopic

Specimen:	(1) 半径(a)范围(nm)	(2) 长度($2L$)范围(nm)
#1, Shangtan, 1200°C	1.8 左右	2.0—5.0*
#2, Shangtan, >2500°C	1.7 左右 (3)	2.5—7.0*
#3, Japan, 1300°C	1.6 左右	2.0—4.5*
#4, Japan, >2500°C	1.8 左右	3.0—6.0*

*Because of the limitations imposed by the scanning angle, holes with a greater length ($2L$) cannot be measured.
Key: (1) Range of radius a (nm); (2) Range of length $2L$ (nm); (3) Approximately.

The experiment was conducted on a diffraction instrument equipped with a Japanese Lixue model 2203E5 small angle scatter installation. Because the smallest scanning angle was about 0.15°, longer needle-form holes could not be measured.

In order to avoid errors that might be occasioned by our illustrations, the authors have prepared a flow chart (Fig. 9) based on the steps discussed above. The flow chart not only can make the choice of a straight line model or a Gauss graph model on the basis of the size of the interrelated coefficient, but it is also able to achieve regressive accuracy and stable parameters, making the entire calculation more elegant and accurate.

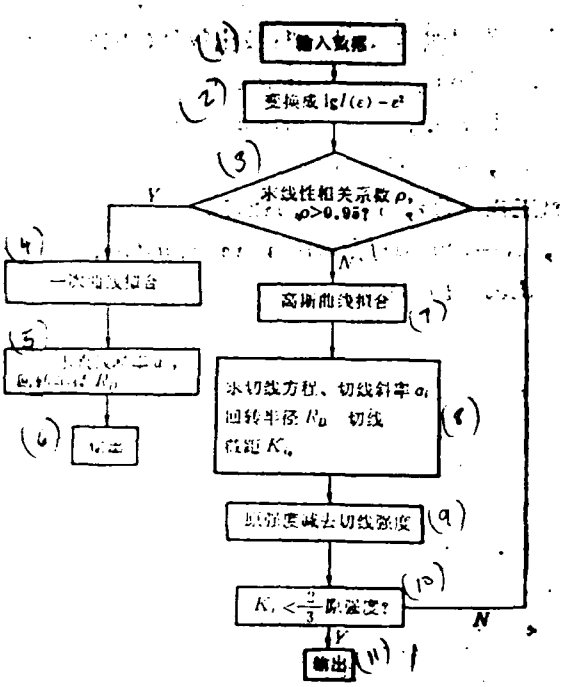

Fig. 9. Calculation flow chart.

Key:
(1) Enter data.
(2) Convert to $\lg I(\varepsilon)-\varepsilon^2$.
(3) Solve for interrelated coefficient ρ. Is ρ >0.95
(4) Linear graph model.
(5) Find straight line slope a; radius of gyration R_D.
(6) Output.
(7) Gauss graph model.
(8) Find tangent formula, tangent slope a_1, radius of gyration R_D, and tangent intersection K_1.
(9) Reduce original intensity by tangent intensity.
(10) Is K_1 <2/3 the original intensity
(11) Output.

4. CONCLUSION

Based on the results of X-ray diffraction analysis, the microscopic structure of carbon fiber can be summed up as follows:

Most carbon fibers belong to the "random-layer graphite" structure class. On the layer surface along the fiber axis there is irregular stacking. Between each layer surface and the fiber axis there exists a certain degree of

orientation. In "graphite random layers" there also exist small, needle-form holes, which are arranged along the axis. Their diameter is in the general range of 1.0 nm to 2.0 nm, their length in the range from 2.0 to several nm.

As the hot processing temperature is raised, the degree of graphitization rises, and the layer surface stacks in the "random-layer graphite" become thicker (the value of L_a and L_c increase). Further, the regularity of the structure increases, the inter-layer distance $d_{(002)}$ gradually approaches the lattice constant ($d_{(002)}$=0.3354 nm) of graphite, and the degree of orientation is reduced. The scale of the fiber-state holes shows some increase, and the anisotropy is apparent.

Literature

1. Johoson [sic], D.J. Carbon fiber. London (1983), 67.
2. Fourdeux, A., R. Perret and W. Ruland. Carbon fibres, their Composites and Applications. The Plastics and [sic] Institute, London (1971), 57.
3. Xu Shunsheng. Jinsu X Shexianxue [Metal X-ray radiography]. Shanghai Science and Technology Press (1962), 304.
4. Johoson, D.J. Carbon fiber. London (1983), 58.
5. Donnet, J.B. and A. Voct. Carbon black. New York (1976).
6. Xiao Lin Hefu. Tansu [Carbon], 60 (1970), 21.
7. Yang Yuxing. Jixie Gongcheng Xuebao [Mechanical Engineering Journal], 18 1(1982), 79.
8. Guinier, A. X-ray diffraction in crystals, imperfect crystals and amorphous bodies (1963), 329.

DISTRIBUTION LIS

DISTRIBUTION DIRECT TO RECIPIENT

ORGANIZATION	MICROFICHE
A205 DMAHTC	1
C509 BALLISTIC RES LAB	1
C510 R&T LABS/AVEADCOM	1
C513 ARRADCOM	1
C535 AVRADCOM/TSARCOM	1
C539 TRASANA	1
C591 FSTC	4
C619 MIA REDSTONE	1
D009 MISC	1
E053 HQ USAF/INET	1
E404 AEDC/DOF	1
E408 AFWL	1
E410 AD/IND	1
F429 SD/IND	1
P005 DOE/ISA/DDI	1
P050 CIA/OCR/ADD/SD	2
AFIT/LDE	1
FTD	
CCV	1
MIA/PHS	1
LLYL/CODE 1-399	1
NASA/NST-44	1
NSA/T513/TDL	2
ASD/FTD/TQLA	1
ESL/NIX-3	1
NOIC/NOIC-09	1